Ab Initio Study of Gas-Phase Proton Transfer in Ammonia−Hydrogen Halides and the Influence of Water Molecules

James A. Snyder, Robert A. Cazar,† Alan J. Jamka, and Fu-Ming Tao*

Department of Chemistry and Biochemistry, California State University, Fullerton, Fullerton, California 92834

Received: June 11, 1999

The gas-phase proton-transfer reaction between ammonia and the hydrogen halides HF, HCl, and HBr and the influence of one, two, and three water molecules are investigated with high-level ab initio calculations on molecular clusters of $NH_3-HX-(H_2O)_n$, $n = 0, 1, 2, 3$ with X = F, Cl, Br. Equilibrium geometries, dissociation energies, HX harmonic frequencies, and potential energy surfaces along the proton-transfer pathway of NH_3-HX are calculated at the second-order Møller−Plesset perturbation (MP2) level with the extended basis set 6-311++G(d,p). It is found that although the NH_3-HX dimer exists as a hydrogen-bonded structure for X = F, Cl, and Br, it can be converted to an ion pair in the presence of water molecules. One water molecule is sufficient to promote a proton transfer from HBr to NH_3, resulting in the ion pair $NH_4^+\cdots Br^-$, whereas at least two water molecules are required to induce a proton transfer from HCl to NH_3. Three water molecules appear to promote a partial proton transfer from HF to NH_3. The potential energy surfaces along the proton-transfer pathway demonstrate the energy difference present between two forms of each cluster in which the NH_3-HX system exists either as a hydrogen-bonded unit or as an ion pair $NH_4^+\cdots X^-$. The successive addition of water molecules to the system gradually increases the stability of the ion pair relative to the hydrogen-bonded form. The potential energy curves, along with the geometry data and HX vibrational frequencies of the clusters, show how the progressive addition of water molecules affects a particular ammonia−hydrogen halide cluster and also indicate what trends exist between different ammonia−hydrogen halide clusters associated with the same number of water molecules.

1. Introduction

The proton transfer between hydrogen halide (HX) and ammonia (NH_3) represents a prototypical acid−base reaction. This is of considerable importance for understanding a variety of processes such as particulate product formation in the atmosphere and chemical reactions in biological systems. In these reactions, the solvent is expected to assume an important role in facilitating proton transfer. In an aqueous or other polar solvent, ionization of NH_3-HX is readily promoted, producing the solvated ionic species $NH_4^+\cdots X^-$. Previous theoretical and experimental studies[1,2] have demonstrated that the gas-phase NH_3-HX system exists as a hydrogen-bonded complex in which HX serves as a hydrogen-bond donor and NH_3 is a hydrogen-bond acceptor. Moreover, self-consistent reaction field (SCRF) calculations predict the existence of the ionic species $NH_4^+\cdots Cl^-$ in an aqueous solvent.[3] In the SCRF models, the solute is placed in a cavity surrounded by a continuum possessing the dielectric permittivity of liquid water. However, no information describing the actual interaction of the water with the solvated complex is provided by such studies.

The stepwise association of single water molecules with the gas-phase complex can eventually facilitate ionization within the complex, producing the $NH_4^+-X^-(H_2O)_n$ cluster. We have previously shown this for the NH_3-HCl system using ab initio calculations.[4] We determined how many water molecules were required to promote the ionization step and deduced what particular geometrical relations might exist between the water and ions within the system, especially in relation to the mechanism of proton transfer.

In this paper, we present the results of high-level ab initio calculations on $NH_3-HX-(H_2O)_n$ clusters for three hydrogen halides HF, HCl, and HBr, with the number of water molecules varying from none to three ($n = 0, 1, 2, 3$). The results include equilibrium geometries, binding energies, HX vibrational stretching frequencies, and the potential energy curves along the NH_3-HX proton-transfer pathway. Of particular interest are the minimum number of water molecules required to promote ionization within the complex and its correlation with the acidity of the HX series. Since the order of acidity among the hydrogen halides increases in the order HF < HCl < HBr, one expects that the propensity for proton transfer between HX and NH_3 in the $NH_3-HX-(H_2O)_n$ complex should follow the same order for a given $NH_3-HX-(H_2O)_n$ complex. Legon et al.[5−7] have concluded that the interaction in NH_3-HX is that of a hydrogen bond on the basis of microwave experiments. These authors also studied proton transfer in numerous other acid−base complexes such as methylated amine−hydrogen halides and found that gas-phase proton transfer was a rare event.[5−7] The successive addition of water molecules to the NH_3-HX system is expected to influence the structure of the system, which is characterized by the hydrogen bond length between the N atom and the H atom bonded to the X halogen atom (H_X). In this study, we examine the effect of varying both the water molecule coordination number ($n = 0, 1, 2, 3$) and the halogen (X = F, Cl, Br) of the hydrogen halide HX within the $NH_3-HX-(H_2O)_n$ complex. The ab initio calculations provide the predicted molecular properties that may be useful in discerning the

† Current address: Department of Chemistry, Polytechnic University of Riobamba, P.O. Box 06-01-178, Riobamba, Ecuador.

10.1021/jp991918j CCC: $18.00
Published on Web 08/31/1999

TABLE 1: Equilibrium Bond Lengths (Å), Bond Angles (deg), and Dipole Moments (D) of the NH_3, NH_4^+, and H_2O Monomers from MP2 Calculations

parameter	MP2	exptl[a]
	NH_3	
R(N−H)	1.014	1.012
∠(HNH)	107.3	106.7
dipole moment	1.74	1.51
	NH_4^+	
R(N−H)	1.025	
∠(HNH)	109.5	
dipole moment	0.001	
	H_2O	
R(O−H)	0.960	0.957
∠(HOH)	103.5	104.5
dipole moment	2.26	1.85

[a] Experimental data from refs 15 and 16.

physical origin of how individual water molecules facilitate proton transfer in general.

2. Computational Details

All equilibrium geometries in this study were determined using full geometry optimization at the level of frozen-core second-order Møller−Plesset perturbation approximation (MP2)[8,9] with the 6-311++G(d,p) extended basis set.[10−12] Harmonic vibrational frequencies corresponding to the equilibrium geometries were also computed at the same level of theory using analytic second-order derivatives of energy with respect to nuclear coordinates. Infrared intensities were calculated using the derivatives of the dipole moment, and subsequent transformation to normal modes.

The dissociation energy, D_e, for a cluster was calculated by taking the difference between the total energy of the cluster and the sum of the total energies of the isolated constituent molecules (HX, NH_3, H_2O) comprising the cluster, that is,

$$D_e = [E(\mathrm{HX}) + E(\mathrm{NH_3}) + nE(\mathrm{H_2O})] - E[\mathrm{NH_3{-}HX{-}(H_2O)_}n] \quad (1)$$

No attempt was made in this study to determine the effect of basis set superposition error (BSSE) on the computed values of D_e. In a previous study,[13] which examined the intermolecular interaction between NH_3 and HNO_3, it was found that the BSSE contribution to the value of D_e at the equilibrium geometry was less than 0.4 kcal mol^{-1}, compared to the value of D_e, which was 14 kcal mol^{-1}. The level of theory and basis set used were comparable to those used in the present study. We assume, therefore, that the BSSE contribution is negligible in this study.

The potential energy surface along the path of proton transfer was calculated for each cluster with the H−X bond length fixed at incremental values while the remaining geometry of the system was optimized.

All calculations were performed using the Gaussian 94 program[14] on a DEC Alpha 5/266 workstation with a Digital UNIX operating system.

3. Results and Discussion

Overview. Table 1 presents equilibrium bond lengths, bond angles, and dipole moments for the NH_3, NH_4^+, and H_2O monomers. Table 2 presents equilibrium bond lengths, bond angles, dipole moments, vibrational frequencies, and IR intensity data for the HX monomers. It is apparent from Tables 1 and 2 that the computed quantities compare well with the corresponding experimental values. The computed bond lengths are within 0.005 Å of the experimental values, and the bond angles agree within 1° of the experimental values. The computed dipole moments, however, are appreciably larger than the experimental values.

TABLE 2: Equilibrium Bond Lengths (Å), Dipole Moments (D), HX Vibrational Stretching Mode Frequencies (cm^{-1}), and IR Adsorption Intensities of the HX Monomers from MP2 Calculations

parameter	MP2	exptl[a]
	HF	
R(H−F)	0.9166	0.9169
dipole moment	1.968	1.826
frequency	4199	4139
intensity	142	
	HCl	
R(H−Cl)	1.2730	1.2746
dipole moment	1.440	1.109
frequency	3091	2989
intensity	35	
	HBr	
R(H−Br)	1.4124	1.4145
dipole moment	1.103	0.827
frequency	2739	2650
intensity	8.5	

[a] Experimental data from ref 17. Experimental values for HX stretching mode frequencies are harmonic frequencies.

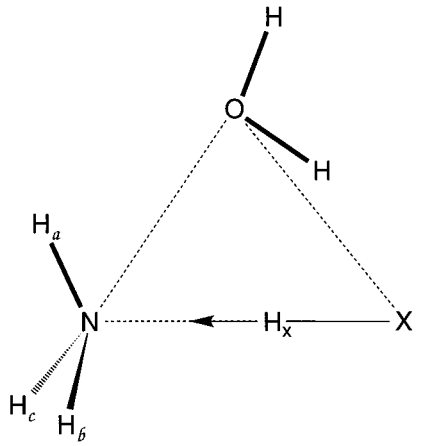

Figure 1. Schematic structure of the NH_3−HX−H_2O cluster and the labeling of the atoms. The cluster structure with two or three H_2O molecules can be generated by orienting each additional H_2O molecule at the remaining C_{3v} symmetry position about the principal axis of NH_3−HX.

Figure 1 displays a schematic geometry of the NH_3−HX−H_2O cluster and indicates how the atoms are labeled. Table 3 provides selected bond lengths, bond angles, dissociation energies, dipole moments, and HX stretching frequencies and the corresponding IR intensities for each of the clusters.

For the NH_3−HX dimer, the HX is oriented along the C_3 axis of the ammonia molecule, producing a structure of C_{3v} symmetry. Incorporation of the first water molecule produces a complex in which the three constituent monomers of the complex are, in general, positioned at the apexes of an equilateral triangle. The C_{3v} symmetry no longer exists in this complex. For the NH_3−HX−$(H_2O)_2$ complex, the second water molecule is positioned at the second symmetry site of NH_3−HX relative to the first water molecule (see Figure 1). Addition of the third molecule restores the C_{3v} symmetry.

NH_3−HX Dimer. Table 3 shows that, for the three NH_3−HX dimers, the bond lengths $R(H_X{-}N)$ are in the range 1.70−1.82 Å. It is apparent that the interaction between HX and NH_3

TABLE 3: Selected Equilibrium Bond Lengths (Å), Dissociation Energies (kcal mol^{-1}), Dipole Moments (D), HX Stretching Mode Frequencies (cm^{-1}), and HX IR Intensites for HX−NH$_3$−(H$_2$O)$_n$ Clusters

	$NH_3-HF-(H_2O)_n$				$NH_3-HCl-(H_2O)_n$				$NH_3-HBr-(H_2O)_n$		
	$n=0$	$n=1$	$n=2$	$n=3$	$n=0$	$n=1$	$n=2$	$n=3$	$n=0$	$n=1$	$n=2$
$R(H_X-X)$	0.948	0.968	1.002	1.264	1.312	1.361	1.861	1.938	1.460	1.933	2.112
$\Delta R(H_X-X)^a$	0.031	0.051	0.085	0.347	0.039	0.088	0.588	0.665	0.048	0.521	0.700
$R(H_X-N)$	1.705	1.611	1.490	1.157	1.820	1.613	1.087	1.062	1.808	1.113	1.065
$R(X-N)$	2.653	2.567	2.483	2.420	3.132	2.966	2.922	3.00	3.268	3.029	3.117
$\angle(H_aNH_b)$	106.8	107.7	108.4	109.2	106.7	108.0	111.5	112.5	106.8	110.2	112.0
D_e	13.4	21.6	28.6	35.8	9.3	17.1	30.4	42.7	8.3	20.5	35.3
dipole moment	4.915	2.757	1.150	1.059	4.648	3.470	6.038	4.181	4.693	8.349	7.170
frequency (ν)	3483	3093	2466	1525	2598	1901			2132		
$\Delta\nu^a$	−716	−1106	−1733	−2674	−563	−1190			−607		
I_{HX}	1470	1904	2404	2508	1572	2887			1775		
I/I_{HX}^a	10	13	17	18	45	83			209		

[a] $\Delta R(H_X-X) = R(H_X-X)_{cluster} - R(H_X-X)_{HX}$. $\Delta\nu = \nu_{cluster} - \nu_{HX}$. $I/I_{HX} = I_{cluster}/I_{HX}$. HX denotes isolated HX monomer.

is that of hydrogen bond resulting from an electrostatic attraction between the nitrogen lone pair and the hydrogen of HX. The hydrogen bond length $R(H_X-N)$ is slightly smaller than that of the water dimer (1.96 Å), implying that a somewhat stronger hydrogen bond exists between NH_3 and HX. Among the three halides, HF appears to have the shortest H_X-N bond length and therefore to form the strongest hydrogen bond with NH_3. Little change in the geometry of the NH_3 unit occurs following complexation. The H_a-N-H_b angle increases by about 2% as a result of complexation. The H_X-X bond length increases by 3.4%, 3.1%, and 3.4% relative to the HX monomer for the NH_3-HX dimers of F, Cl, and Br, respectively. Such small changes are indicative of the remaining but weakened covalent bond for HX and are consistent with a hydrogen-bonded structure for the dimer complexes.

The strength of the hydrogen bond in NH_3-HX can be quantified by the dissociation energy of NH_3-HX. As shown in Table 3, the dissociation energy decreases in the order F > Cl > Br. The order of decreasing dissociation energy and increasing H_X-X bond length appears to follow the expected trend when compared with the hydrogen halide dipole moment in the series (HF > HCl > HBr). The magnitude of the dissociation energy for the NH_3-HF dimer is about 4 kcal mol^{-1} larger than that for the NH_3-HCl dimer, which, in turn, is only 1.0 kcal mol^{-1} larger than that of the NH_3-HBr dimer. On the other hand, the dissociation energy is also expected to be dependent on the acidity of HX. The HX with higher acidity would promote the stronger hydrogen bond interaction with NH_3 and in turn would give a larger dissociation energy for NH_3-HX. Surprisingly, the calculated dissociation energies of NH_3-HX are in exactly opposite order of the HX acidity in the series (HF < HCl < HBr). This result shows that the strength of the hydrogen bond in NH_3-HX is primarily determined by electrostatic interactions, dominated by the dipole−dipole interaction, rather than the acidity of HX.

The change in the HX covalent bond upon the formation of hydrogen bond with NH_3 may be exhibited by the change in the HX stretching frequency. As shown in Tables 2 and 3, the HX vibrational frequencies in NH_3-HX are decreased, or red-shifted, from that of the isolated HX monomer, accompanied by a large increase in the IR intensity. The magnitude of the red shift and the change in the IR intensity are consistent with the weakening of the HX bond as the HX bond distance is lengthened in NH_3-HX. The red shifts are on the order of 500−700 cm^{-1}, indicating substantial weakening of the HX covalent bond in the formation of hydrogen bond in NH_3-HX. The IR intensities for the dimers increase by 10-, 45-, and 200-fold for NH_3-HF, NH_3-HCl, and NH_3-HBr, respectively. The IR intensity is proportional to the dipole moment enhancement upon the HX stretch, and the large increases in the IR intensity reflect the fact that the presence of NH_3 dramatically induces such an enhancement in NH_3-HX. The intensity increases appear to correlate well with the increases in the dipole moment of NH_3-HX from that of free HX, 2.94, 3.21, and 3.59 D for NH_3-HF, NH_3-HCl, and NH_3-HBr, respectively. All these results indicate that the HX bond polarity increases as the HX covalent bond weakens upon the formation of hydrogen bond in NH_3-HX, and such an effect follows in the order HF < HCl < HBr.

NH_3-HX-H_2O. The effects of complexing one water molecule with NH_3-HX to produce NH_3-HX-H_2O are discussed next. Relative to the isolated HX monomer, the HX bond length increases by 5.5%, 7%, and 36.8% for the NH_3-HX-H_2O clusters of F, Cl, and Br, respectively. The increases in the HF and HCl bond lengths indicate the further weakening of the covalent bond in the clusters upon the addition of a water molecule. On the other hand, the increase in the HBr bond length relative to the free HBr monomer is 0.048 and 0.521 Å for NH_3-HBr and $NH_3-HBr-H_2O$, respectively. The H_X-Br distance in $NH_3-HBr-H_2O$ is 1.933 Å. The abrupt increase for the monohydrated cluster implies that the covalent HBr bond is no longer in existence and the water molecule has a more pronounced effect on the dissociation of H_X from Br. Moreover, the $N-H_X$ distance decreases from 1.808 Å in NH_3-HBr to 1.113 Å in $NH_3-HBr-H_2O$. The latter is comparable to a typical N−H bond length in NH_4^+. This indicates that proton transfer has taken place between HBr and NH_3 in $NH_3-HBr-H_2O$.

As can be seen from Table 3, the incorporation of one water molecule into the system is accompanied by a decrease in the dipole moment by 2.2 D for NH_3-HF-H_2O and 1.2 D for $NH_3-HCl-H_2O$, whereas for $NH_3-HBr-H_2O$, the dipole moment increases by 3.7 D. The decreases for NH_3-HF-H_2O and $NH_3-HCl-H_2O$ are due to the partial cancellation of the component vectors by that of the water molecule. A plausible explanation for the increase for $NH_3-HBr-H_2O$ is the partial cancellation of the component vectors by the water molecule that is not enough to offset the dipole increase due to the formation of an ion pair resulting from proton transfer.

The increase in the dissociation energy for each of NH_3-HF-H_2O and $NH_3-HCl-H_2O$ is about 8 kcal mol^{-1} relative to NH_3-HF and NH_3-HCl, respectively. However, for $NH_3-HBr-H_2O$ the dissociation energy increases by nearly 12 kcal mol^{-1}. The larger increase in the dissociation energy for $NH_3-HBr-H_2O$ can be attributed to more favorable interactions of the ionic species $NH_4^+\cdots Br^-$ with the water molecule than that of a neutral NH_3-HF or NH_3-HCl.

The HX stretching frequencies are further red-shifted for the F and Cl monohydrated clusters from those for the NH_3-HX

dimers, along with large enhancements in the IR intensity. This is correlated with the weakening of the H_X-X bond as the bond distance is lengthened because of the presence of the water molecule. It should be noted that the HBr stretching mode is no longer present because of the ionic dissociation of HBr in the monohydrated cluster. The red shift for the monohydrated Cl cluster is 1190 cm^{-1}, and the IR intensity increases by about 80-fold relative to that of the free HCl monomer. This can be compared to the F cluster, for which the red shift is 1106 cm^{-1}, but the IR intensity increases by only 13-fold relative to that of the free HF monomer. Therefore, the weakening of the H_X-X bond is greater in $NH_3-HCl-H_2O$ than in NH_3-HF-H_2O.

Evidently, the addition of a single water molecule is sufficient to promote proton transfer between HBr and NH_3 in $NH_3-HBr-H_2O$, while for NH_3-HF-H_2O and $NH_3-HCl-H_2O$, the NH_3-HX unit remains hydrogen-bonded. HBr is the strongest acid among the series HF, HCl, HBr, and it is therefore reasonable that the ionic dissociation happens first with HBr. It is interesting to appreciate the significant effect of a single H_2O molecule that is enough to facilitate a complete proton transfer in $NH_3-HBr-H_2O$. For the weaker acid, HF or HCl, the effect of a single water molecule is noticeable on a series of properties, although it is still insufficient to induce a complete proton transfer.

$NH_3-HX-(H_2O)_2$. The addition of a second water molecule to the system has interesting consequences. As Table 3 shows, the dipole moment for $NH_3-HCl-(H_2O)_2$ increases by about 2.5 D compared to the monohydrated cluster. By contrast, the dipole moment for $NH_3-HF-(H_2O)_2$ decreases relative to the monohydrated cluster. For $NH_3-HF-(H_2O)_2$, further cancellation of the dipole component vectors following addition of a second water molecule accounts for this decrease. For $NH_3-HCl-(H_2O)_2$, the dipole moment increase can be attributed to formation of an ion pair as a result of proton transfer from HX to NH_3. For $NH_3-HBr-(H_2O)_2$, the dipole moment decreases by 1.1 D relative to the monohydrated cluster, and the decrease is attributed to cancellation of the dipole component vectors by the second water molecule.

The changes in the H_X-X bond lengths in $NH_3-HX-(H_2O)_2$ relative to the isolated HX monomer are 9%, 46%, and 50% for X = F, Cl, and Br, respectively. Moreover, the largest change in the H_X-X bond length relative to the monohydrated system occurs for $NH_3-HCl-(H_2O)_2$. The increase in the H_X-Cl bond lengths relative to the bond length of the free HCl monomer are 0.088 and 0.588 Å for the $NH_3-HCl-H_2O$ and $NH_3-HCl-(H_2O)_2$ clusters, respectively. This greater increase in the H_X-Cl bond length accompanying the addition of the second water molecule indicates that the second water molecule produces a unique effect within the cluster system compared with addition of the first water molecule. For $NH_3-HCl-(H_2O)_2$, the H_X-Cl distance is 1.861 Å and the H_X-N distance is 1.087 Å, consistent with H_X-Cl bond breakage and the formation of NH_4^+ by a proton (H_X) transfer to NH_3. For $NH_3-HF-(H_2O)_2$, addition of the second water molecule does not appear to promote proton transfer. The H_X-F bond distance is 1.002 Å and the H_X-N distance is 1.49 Å, which is still characteristic of a hydrogen-bonded structure.

The dissociation energies for the $NH_3-HCl-(H_2O)_2$ and $NH_3-HBr-(H_2O)_2$ clusters are 30.4 and 35.3 kcal mol^{-1}, respectively. The magnitudes of these values have increased by approximately 15 kcal mol^{-1} relative to the values for the respective monohydrated clusters. By comparison, the dissociation energy for the $NH_3-HF-(H_2O)_2$ is 28.59 kcal mol^{-1}, which represents an increase in magnitude of about 7 kcal mol^{-1} relative to the NH_3-HF-H_2O cluster. It follows that for $NH_3-HCl-(H_2O)_2$ and $NH_3-HBr-(H_2O)_2$, the second water molecule provides greater stabilization of the clusters owing to favorable interactions of water with the ion pair $NH_4^+\cdots X^-$ in the clusters. The absence of such an ion pair in $NH_3-HF-(H_2O)_2$ means less favorable interactions with the second water molecule, causing a smaller increase in the dissociation energy.

The H_X-F stretching frequency is further red-shifted as a result of the weakening of the covalent bond due to the addition of the second water molecule. The red shift from the free HF monomer is 1733 cm^{-1} for the dihydrated cluster, which is compared with a red shift of 1106 cm^{-1} for the monohydrated cluster and 716 cm^{-1} for the NH_3-HF dimer. As expected, the IR intensity is also enhanced by the addition of the second water. This gradual increase in the red shift, along with the enhancement in the IR intensity, is consistent with the weakening of the H_X-F covalent bond and the increase of the bond polarity with successive addition of water molecules in the clusters. No HX stretching frequencies are reported for $NH_3-HCl-(H_2O)_2$ and $NH_3-HBr-(H_2O)_2$, since proton transfer has occurred in these clusters.

$NH_3-HX-(H_2O)_3$. The effects due to the presence of a third water molecule within the complex can be seen from Table 3. Again, we can start with the dipole moment. For the $NH_3-HF-(H_2O)_3$ and $NH_3-HCl-(H_2O)_3$ complexes, the dipole moment decreases by 0.09 and 1.9 D, respectively, compared with the values for the dihydrated clusters. The decrease can be understood as arising from a restoration of the C_{3v} symmetry of the cluster following addition of the third water molecule and from a resulting partial cancellation of dipole moment vector components. The smaller decrease for $NH_3-HF-(H_2O)_3$ relative to the dihydrated complex is expected if some partial charge transfer occurs following addition of a third water molecule.

The H_X-F bond length in the $NH_3-HF-(H_2O)_3$ complex is 1.264 Å, an increase of 37.8% relative to the isolated HF monomer. The H_X-F bond length is increased from 1.002 Å for $NH_3-HF-(H_2O)_2$. On the other hand, the H_X-N distance is decreased from 1.490 to 1.157 Å. The geometrical changes indicate that the presence of the third water molecule has promoted at least a partial proton transfer between HF and NH_3 in the trihydrated cluster.

Relative to the dihydrated Cl cluster, which already exist as an ion pair system, the changes in geometry accompanying the addition of the third water molecule are not as pronounced compared with the changes that follow addition of the second water molecule to form the dihydrated cluster. The H_X-Cl bond distance increases by an additional 0.077 Å, and the $N-H_X$ distance decreases by 0.027 Å. Hence, for $NH_3-HCl-(H_2O)_3$, the function of a third water molecule is primarily to provide further stabilization of the charged pair species.

The HF stretching frequency in $NH_3-HF-(H_2O)_3$ is red-shifted by 2674 cm^{-1} from the HF monomer, which is the largest compared to the shifts for NH_3-HF, NH_3-HF-H_2O, and $NH_3-HF-(H_2O)_2$. This is consistent with the largest increase in the H_X-F bond length for the trihydrated cluster. The enhancement in the IR intensity increases monotonically from 10- to 18-fold as water molecules are progressively added to NH_3-HF.

The dissociation energy increases from 28.6 kcal mol^{-1} for $NH_3-HF-(H_2O)_2$ to 35.8 kcal mol^{-1} for $NH_3-HF-(H_2O)_3$, resulting in a net increase of about 7 kcal mol^{-1} due to the addition of the third water. By contrast, the dissociation energy increases from 30.4 kcal mol^{-1} for $NH_3-HCl-(H_2O)_2$ to 42.7 kcal mol^{-1} for NH3−HCl−$(H_2O)_3$, a change of about 12 kcal mol^{-1}. Again, the larger increase for the Cl cluster is likely

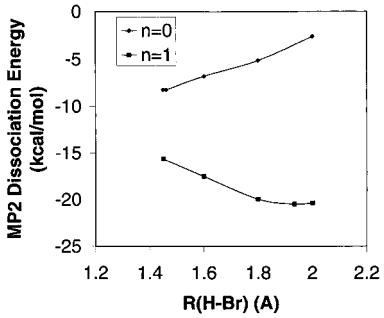

Figure 2. Potential energy surfaces of the $NH_3-HF-(H_2O)_n$ complex along the $R(H_X-F)$ coordinate.

TABLE 4: Approximate Slope Values (kcal mol^{-1} Å^{-1}) for Potential Energy Curves between Points on the Curve That Correspond Approximately to a Hydrogen-Bonded Structure and a Structure in Which the $NH_4^+-X^-$ Ion Pair Exists for Each of the $NH_3-HX-(H_2O)_n$ Clusters

n	$NH_3-HF-(H_2O)_n$	$NH_3-HCl-(H_2O)_n$	$NH_3-HBr-(H_2O)_n$
0	59	21	9
1	34	3	−12
2	13	−15	
3	−10		

due to more favorable interactions of the third water with the $NH_4^+\cdots Cl^-$ ionic pair. The smaller increase for the F cluster supports the conclusion that complete formation of the $NH_4^+\cdots F^-$ ionic pair in $NH_3-HF-(H_2O)_3$ is not yet attained.

Potential Energy Surfaces. Further insights into the nature of the proton transfer between NH_3 and HX can be obtained by examining the potential energy surface traversing the space over which a proton transfer occurs from HX to NH_3. The potential energy curves for the various clusters are plotted in Figures 2−4.

Comparison of the curves for the NH_3-HX dimers shows that the potential energy minima occur at $R(H_X-X)$ values of 0.948, 1.312, and 1.46 Å, for X = F, Cl, and Br, respectively. These values are characteristic of hydrogen-bonded structures. One might expect a second minimum that corresponds to the ion pair $NH_4^+\cdots X^-$ that results from a proton transfer in NH_3-HX. Such a second minimum never occurs, and the potential energy curve rises monotonically beyond the H_X-X equilibrium distance in each of the NH_3-HX dimers. For the hydrated clusters, the potential energy curves each maintain a single minimum that is shifted to a larger H_X-X distance. The overall difference in the potential energy curves for each series $NH_3-HX-(H_2O)_n$ appears to be the declining slope with the increasing number of water molecules.

To make the comparison of the curves more quantitative, approximate values for the slopes of the potential energy curves have been calculated. These values are tabulated in Table 4. The slope values are computed by first taking the difference in energy between points on the curves corresponding, approximately, to where a hydrogen-bonded structure exists and where a structure composed of the $NH_4^+\cdots X^-$ ion pair should exist. This difference is then divided by the difference between the respective $R(H_X-X)$ values for the two points. For NH_3-HX dimers, the slopes are 59, 21, and 9 kcal mol^{-1} Å^{-1} for NH_3-HF, NH_3-HCl, and NH_3-HBr, respectively. That is, the steepest curve is that of the NH_3-HF dimer but becomes progressively flatter for the NH_3-HCl and NH_3-HBr dimers (Figures 3 and 4). Hence, the energy difference between hydrogen-bonded and ion pair structures is greatest for the NH_3-HF dimer and smallest for the NH_3-HBr. We therefore conclude that the relative propensity toward proton transfer

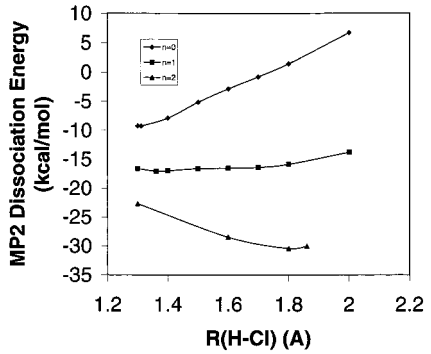

Figure 3. Potential energy surfaces of the $NH_3-HCl-(H_2O)_n$ complex along the $R(H_X-Cl)$ coordinate.

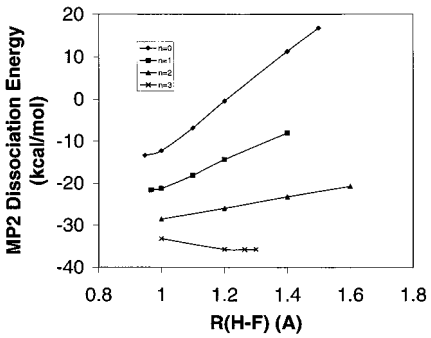

Figure 4. Potential energy surfaces of the $NH_3-HBr-(H_2O)_n$ complex along the $R(H_X-Br)$ coordinate.

within the NH_3-HX dimer increases in the order NH_3-HF < NH_3-HCl < NH_3-HBr.

To understand the effects following the addition of the first water molecule, the slope values in the first and second rows of Table 4 can be compared. The slope of the curves decrease from 59 to 34 kcal mol^{-1} Å^{-1} for NH_3-HF-H_2O, from 21 to 3 kcal mol^{-1} Å^{-1} for $NH_3-HCl-H_2O$, and from 9 to −12 kcal mol^{-1} Å^{-1} for $NH_3-HBr-H_2O$. It follows that the addition of the water molecule has reduced the difference in energy between the hydrogen-bonded complex and the ionized structure for each of the NH_3-HX-H_2O complexes. However, for NH_3-HF-H_2O and $NH_3-HCl-H_2O$, the minima occur at $R(H_X-X)$ values of 0.968 and 1.361 Å, respectively, which still correspond to values characteristic of hydrogen-bonded structures. For $NH_3-HBr-H_2O$, the slope changes to a negative value and the minimum occurs at $R(H_X-X)$ = 1.933 Å, which indicates a structure containing an ionic pair, $NH_4^+-Br^-$.

Hence, the potential energy curves for proton transfer between HX and NH_3 indicate that proton transfer is favored in $NH_3-HBr-H_2O$ but not in NH_3-HF-H_2O or $NH_3-HCl-H_2O$. However, proton transfer is made more energetically feasible in NH_3-HF-H_2O and $NH_3-HCl-H_2O$ relative to the NH_3-HX dimers, since the curves become flatter following the addition of one water molecule.

The potential energy curves for the dihydrated clusters change further from those for the monohydrated clusters. For $NH_3-HCl-(H_2O)_2$, a minimum occurs at $R(H_X-Cl)$ = 1.861 Å corresponding to an ion pair structure, while a hydrogen-bonded structure should occur near $R(H_X-Cl)$ = 1.35 Å. The latter is about 8 kcal mol^{-1} higher in energy than the former. From Table 4, it is seen that the slope decreases from 3 kcal mol^{-1} Å^{-1} for $NH_3-HCl-H_2O$ to −15 kcalmol^{-1} Å^{-1} for $NH_3-HCl-(H_2O)_2$. Similarly, the slope decreases from 34 kcal mol^{-1} Å^{-1} for NH_3-HF-H_2O to 13 kcal mol^{-1} Å^{-1} for $NH_3-HF-(H_2O)_2$. It is evident, therefore, that the second water molecule promotes

proton transfer in $NH_3-HCl-(H_2O)_2$ but does not completely facilitate proton transfer within the $NH_3-HF-(H_2O)_2$ system.

The potential energy curve for $NH_3-HF-(H_2O)_3$ is even flatter than that of the dihydrated cluster. The slope decreases from 13 to -10 kcal mol^{-1} Å^{-1} by the addition of the third water molecule. This implies that proton transfer has taken place in $NH_3-HF-(H_2O)_3$. However, the potential minimum occurs at $R(H_X-F) = 1.264$ Å, which still corresponds to a geometry that is between the geometries of hydrogen-bonded and ion pair forms.

The conclusions obtained from the analysis of the potential energy curves complement the findings of the previous section on the basis of changes in the H_X-X bond length and accompanying vibrational frequency shifts for the $NH_3-HX-(H_2O)_n$ complexes. Comparing the slopes of the curves for the various clusters shows that the incremental addition of water molecules to the ammonia−hydrogen halide system progressively reduces the difference in energy separating hydrogen-bonded and ion pair structures.

It is interesting to note the relationship among the values in Table 4 between successive rows. For each $NH_3-HX-(H_2O)_n$, the addition of one water molecule appears to decrease the slope by about 20 kcal mol^{-1} Å^{-1}. Therefore, the possibility may exist for predicting how many water molecules might be required to induce proton transfer in $NH_3-HX-(H_2O)_n$, based only on the slope of the potential energy curve for the NH_3-HX dimer. If the slope for NH_3-HX is between 0 and 10 kcal mol^{-1} Å^{-1}, as in the case of NH_3-HBr, one water molecule would be enough to make the slope negative and to induce proton transfer. If the slope is near 20 kcal mol^{-1} Å^{-1}, as for NH_3-HCl, it is likely that two water molecules would be required to promote proton transfer. This apparent correlation offers compelling incentive for further investigations of proton-transfer reactions of other hydrogen-bonded systems.

4. Conclusion

We have reported the results of high-level ab initio calculations on the $NH_3-HX-(H_2O)_n$ clusters with the water molecule coordination number $n = 0$, 1, 2, and 3 and the hydrogen halide HX = HF, HCl, and HBr. The equilibrium structures, H_X-X stretching frequencies, dipole moments, dissociation energies of the clusters, and the potential energy curves along the proton-transfer path from HX to NH_3 have been calculated at the MP2 level using the extended basis set 6-311++G(d,p).

The results of this study show that a predictable trend exists among the hydrogen halide series in the $NH_3-HX-(H_2O)_n$ system, with respect to propensity toward proton transfer between gas-phase HX and NH_3, facilitated by 0, 1, 2, or 3 water molecules. The successive addition of water molecules to complexes of NH_3 and HX gradually weakens the H_X-X bond. Proton transfer from HBr to NH_3 is readily promoted with the addition of a single water molecule to the complex $HBr-NH_3$. Proton transfer between HCl and NH_3 apparently requires two water molecules, while proton transfer between HF and NH_3 requires at least three water molecules. These results are consistent with the known trend in the acidity of the HX series, which increases in the order HF < HCl < HBr.

Potential energy curves along the path of proton transfer from HX to NH_3 were compared, supporting the above conclusions. The successive addition of water molecules to the hydrogen-bonded NH_3-HX system progressively reduces the energy of the structure representing an ion pair with respect to the hydrogen-bonded structure. Such effects are quantified by the slopes of the potential energy curves between the points corresponding to the hydrogen-bonded structure and the structure representing an ion pair. For given hydrogen halide, the slope decreases by approximately 20 kcal mol^{-1} Å^{-1} for each addition of one water molecule to the cluster. This may imply that it is possible to predict the minimum number of water molecules required to promote proton transfer in the hydrogen-bonded NH_3-HX system on the basis of the initial slope determined for the NH_3-HX system. The results of this study offer promise for investigating the solvent effect on proton-transfer reactions in larger and more complicated systems.

Acknowledgment. This work was supported by The Petroleum Research Fund (Grant No. 30399-GB6), The Research Corporation (CC4713), and School of Natural Sciences and Mathematics, California State University, Fullerton.

References and Notes

(1) Latajka, Z.; Scheiner, S.; Ratajczak, H. *Chem. Phys. Lett.* **1987**, *135*, 367.

(2) Corongiu, G.; Estrin, D.; Murgia, G.; Paglieri, L.; Pisani, L.; Valli, G.; Suzzi; Watts, J. D.; Clementi, E. *Int. J. Quantum. Chem.* **1996**, *59*, 119.

(3) Chipot, C.; Rinaldi, D.; Rivail, J.-L. *Chem. Phys. Lett.* **1992**, *191*, 287.

(4) Cazar, R. A.; Jamka, A. J.; Tao, F.-M. *J. Phys. Chem. A* **1998**, *102*, 5117.

(5) Legon, A. C.; Rego, C. A. *J. Chem. Phys.* **1989**, *90*, 6867.

(6) Legon, A. C.; Wallwork, A. L.; Rego, C. A. *J. Chem. Phys.* **1990**, *92*, 6397.

(7) Legon, A. C.; Rego, C. A. *J. Chem. Phys.* **1993**, *99*, 1463.

(8) Møller, C.; Plesset, M. S. *Phys. Rev.* **1934**, *46*, 618.

(9) Binkley, J. S.; Pople, J. A. *Int. J. Quantum Chem.* **1975**, *9*, 229.

(10) McLean, A. D.; Chandler, G. S. *J. Chem. Phys.* **1980**, *72*, 5639.

(11) Krishnan, R.; Binkley, J. S.; Seeger, R.; Pople, J. A. *J. Chem. Phys.* **1980**, *72*, 650.

(12) Clark, T.; Chandrasekhar, J.; Spitznagel, G. W.; Schleyer, P. v. R. *J. Comput. Chem.* **1983**, *4*, 294.

(13) Nguyen, M.-T.; Jamka, A. J.; Cazar, R. A.; Tao, F.-M. *J. Chem. Phys.* **1997**, *106*, 8710.

(14) Frisch, M. J.; Trucks, G. W.; Schlegel, H. B.; Gill, P. M. W.; Johnson, B. G.; Robb, M. A.; Cheeseman, J. R.; Keith, T.; Petersson, G. A.; Montgomery, J. A.; Raghavachari, K.; Al-Laham, M. A.; Zakrzewski, V. G.; Ortiz, J. V.; Foresman, J. B.; Cioslowski, J.; Stefanov, B. B.; Nanayakkara, A.; Challacombe, M.; Peng, C. Y.; Ayala, P. Y.; Chen, W.; Wong, M. W.; Andres, J. L.; Replogle, E. S.; Gomperts, R.; Martin, R. L.; Fox, D. J.; Binkley, J. S.; Defrees, D. J.; Baker, J.; Stewart, J. P.; Head-Gordon, M.; Gonzalez, C.; Pople, J. A. *Gaussian 94*, revision D.3; Gaussian, Inc.: Pittsburgh, PA, 1995.

(15) Callomon, J. H.; Hirota, E.; Kuchitsu, K.; Lafferti, W. J.; Makli, A. G.; Pote, C. S. *Structure Data on Free Polyatomic Molecules*; Springer: Berlin, 1976.

(16) Huber, K. P.; Herzberg, G. *Molecular Spectra and Molecular Structure, IV. Constants of Polyatomic Molecules*; van Nostrand Reinhold Company: New York, 1979.

(17) *CRC Handbook of Chemistry and Physics*, 77th ed.; Lide, D. R., Ed.; CRC Press: Boca Raton, FL, 1997.